European Journal of Pharmaceutical Sciences 154 (2020) 105505

Contents lists available at ScienceDirect

European Journal of Pharmaceutical Sciences

journal homepage: www.elsevier.com/locate/ejps

The impact of the degree of intimate mixing on the compaction properties of materials produced by crystallo-co-spray drying

Alan F. McDonagh[a,b], Bronagh Duff[a], Lorna Brennan[a], Lidia Tajber[a,b,*]

[a] School of Pharmacy and Pharmaceutical Sciences, Trinity College Dublin, Dublin 2, Ireland
[b] Synthesis and Solid State Pharmaceutical Centre, Ireland

ARTICLE INFO

Keywords:
Paracetamol
Lactose
Crystallo-co-spray drying
Compressibility
Compactibility
Properties of tablets

ABSTRACT

Direct compression remains one of the most favourable methods available to produce tablet compacts due to its simplicity, efficiency and cost effectiveness however, the technique still remains unsuitable for the majority of formulations due to materials exhibiting poor physical properties such as inadequate compressibility and deformation mechanisms. Whereas crystallo-co-spray drying of various blends has shown to improve the tabletting properties of poorly processable materials, the role of the solvent feed composition in altering the soluble fraction ratio of the excipient to the drug in a crystallo-co-spray dried agglomerate is not well understood. The aim of this work was to investigate the role of the soluble fraction of a drug (paracetamol) and an excipient (α-lactose monohydrate) on the tabletting properties of their crystallo-co-spray dried agglomerates produced via co-spray drying using various inlet feed solvent compositions in order to vary the soluble fraction of the excipient in the feed. It was found that an increase in excipient soluble fraction in the inlet feed resulted in a greater degree of intimate mixing in the final spray dried powder blend, which in turn led to an improvement in tabletting properties of the poorly processable drug.

1. Introduction

Direct compression is regarded as one of the most promising approaches to tablet manufacture due to its lack of laborious steps such as those involved in wet and dry granulation (Chauhan et al., 2017). It is a process in which tablets are compressed directly from powder blends without any prior pre-treatment meaning that it is simple, quick and cost-effective (Gohel and Jogani, 2005; Shangraw, 1993). It is the most preferred method for tablet manufacture, however only a small number of pharmaceutical blends can utilise this method due to unfavourable characterises such as poor compaction behaviour (Shangraw, 1989). In recent years the area of crystallo-co-agglomeration has gained increased interest as a method of improving the tabletting properties of materials (Maghsoodi et al., 2008; Paradkar and Pawar, 2014). Through the use of a “good solvent” into which the drug is soluble, and a “bad solvent” to act as an antisolvent to induce nucleation and growth, a spherical agglomerate of the drug and diluents such as talc, sodium starch glycolate, and starch will be produced using a bridging liquid (Paradkar and Pawar, 2014; Pawar et al., 2004). The concept of crystallo-co-agglomeration has successfully been translated to spray drying to produce crystalline agglomerates of a drug and an excipient with the exception that instead of a bridging liquid being required for agglomerate formation, the diffusion of the components of an atomised droplet towards the centre of the droplet was instead utilised (McDonagh and Tajber, 2020).

Continuous processing has become more and more popular in the pharmaceutical industry in recent years due to the premise of lower running costs, such as reduced capital investment, reduction in labour cost, less required floor space and minimal material wastage as well as faster product output (Vervaet and Remon, 2005; Lindberg, 1988). It is advantageous over traditional batch processes due to the reduction in time-to-market as a result of scale up benefits and better quality (Vervaet and Remon, 2005; H. Leuenberger, 2001; H. Leuenberger, 2001). Spray drying is one such process. It is a fast, versatile technique with a one step process capable of producing a range of particles based on the nature of the material to be dried and spray dryer parameters chosen (Broadhead et al., 1992). The technique is scalable with the ability to modify the physical form of excipients and drugs, capable of improving the material's physiochemical properties such as compressibility and compactibility (Mangal et al., 2015). However, as the flowability of a powder material is subject to the material's density, size and shape (Kaerger et al., 2004), it is common for spray dried materials to exhibit poor flowability. As previously demonstrated, the morphology and size of spray dried paracetamol (PAR) can be controlled

* Corresponding author at: School of Pharmacy and Pharmaceutical Sciences, Trinity College Dublin, College Green, Dublin 2, Ireland.
E-mail address: ltajber@tcd.ie (L. Tajber).

https://doi.org/10.1016/j.ejps.2020.105505
Received 31 March 2020; Received in revised form 28 July 2020; Accepted 4 August 2020
Available online 07 August 2020

through the careful selection of spray dryer operating parameters based on the atomised droplet's characteristics (McDonagh and Tajber, 2019), and in another study, the degree of component mixing in a crystallo-co spray dried agglomerated powder blend was tailored though the selection of the excipients soluble fraction in the inlet feed (McDonagh and Tajber, 2020).

The compression of commercial PAR and molecules of similar tabletting characteristics is a significant issue that the pharmaceutical industry faces. PAR crystals can exist in three polymorphic forms; form I (monoclinic), form II (orthorhombic) and form III (triclinic). Form I is the commercial form of PAR and is the most thermodynamically stable at room temperature but has poor tableting properties and is prone to capping due to its rigid crystal lattice structure and high elastic deformation tendency as a result of the 'zig zag' layered arrangement of the PAR molecules held together by strong hydrogen bonds (Govedarica et al., 2009; Ahmed et al., 2017). In order to improve this, poorly processable drugs are processed with a range of excipients to masque the material's unfavourable characteristics (Huang et al., 2015; Pingali et al., 2011). The choice of excipients is therefore critical in the formulation of directly compressed tablets, most notably the filler-binder. The roles of the filler-binder include improving compactibility, and to bulk up the formulation to produce a conveniently sized tablet (Aulton and Taylor, 2017). α-lactose monohydrate (Lα•H_2O) is widely used in pharmaceutical formulations due to its high stability, non-hygroscopic nature and low cost (Gohel and Jogani, 2005). It is the crystalline Lα•H_2O that is usually used in direct compression processes due to its favourable flowability (Gad, 2008). Lα•H_2O deforms by a combination of particle fracture and plastic deformation (Roberts and Rowe, 1985). Gunsel and Lachman found that spray dried Lα•H_2O produces harder, less friable tablets when compacted (Gunsel and Lachman, 1963), this improvement in tabletability makes spray dried Lα•H_2O an ideal candidate for direct compression.

The area of co-spray drying to improve the physical properties of tablets of various excipient mixtures is well established (Gohel and Jogani, 2005; Rojas et al., 2012). For example StarLac, a co-processed excipient by Meggle Excipients & Technology consisting of Lα•H_2O and maize starch which is produced by co-spray drying shows improved compressibility and disintegration times (Meggle, 2014). This is also true for drug-excipient blends. Gonnissen at al. studied the co-spray drying of PAR with a range of excipients and investigated the blend's flowability, yield and disintegration time (Gonnissen et al., 2008). In a separate study Gonnissen at al. co-spray dried PAR with a range of carbohydrates and investigated the blend's hygroscopicity, flowability, and compactibility (Gonnissen et al., 2007). Al-Zoubi et al. co-spray dried metformin hydrochloride with various polymers leading to improvements in compactibility and tabletability (Al-Zoubi et al., 2017).

We have shown recently that in crystallo-co spray drying the inlet feed composition had the most pronounced impact on the morphology of the agglomerates (McDonagh and Tajber, 2020). However, this effect of excipient to drug soluble fraction in the feed and the resulting variability in the degree of intimate mixing on the physical properties of their respective tablets has not been studied. The aim of this study was therefore to investigate the compaction properties of PAR/Lα•H_2O agglomerates produced through the new process of crystallo-co-spray drying with particular focus on the role of the soluble fraction of the excipient in the spray dryer inlet feed, to produce a material with improved physiochemical characteristics to allow for direct compression to be utilised.

2. Materials and methods

2.1. Materials

Paracetamol (PAR, batch number 078K0032), α-lactose monohydrate (Lα·H_2O, lot number SLBX2254), magnesium stearate (powder), sodium hydroxide and monobasic potassium phosphate were obtained from Sigma-Aldrich (Ireland). Ethanol (EtOH, technical grade) was purchased from T.E Laboratories (Ireland), and deionised water was produced using a Millipore Elix 3 system (Millipore, Saint-Quentin, France).

2.2. Methods

2.2.1. Preparation of powders

2.2.1.1. Crystallo-co spray drying of PAR + Lα·H_2O. Crystallo-co spray dried (CC-SD) samples were prepared as described previously (McDonagh and Tajber, 2020). A series of 10% w/v PAR + Lα·H_2O suspensions in equal weight ratios were made up at different solvent compositions (S_c): 100% EtOH (#1), 90/10% v/v EtOH/H_2O (#2), 80/20% v/v EtOH/H_2O (#3), 70/30% v/v EtOH/H_2O (#4), 60/30% v/v EtOH/H_2O (#5) and 50/50% v/v EtOH/H_2O (#6) and SD using a Büchi B-290 mini spray dryer (Switzerland). The suspensions were stirred using a magnetic stirrer to maintain homogeneity before being fed into a 2-fluid atomising spray nozzle with a 0.7 mm cap. The inlet feed was kept at room temperature and fed into the spray dryer through an incorporated peristaltic pump at approximately 9 mL/min (setting: 30%) with an aspirator drying air flow rate of 38 m^3/h (setting: 100%) and flow metre spraying flow rate of 475 L/h (height: 40 mm) (McDonagh and Tajber, 2020; McDonagh and Tajber, 2019). The drying gas used was air and the dispersant spraying gas was nitrogen. The dried materials were collected from the collection vessel only and were thoroughly mixed using a spatula prior to refrigerated storage (4 ± 1 ^{0}C) in 15 mL amber powder bottles. The spray dryer inlet temperature was kept constant at 120 °C and all samples were SD in triplicate.

2.2.1.2. Spray drying of PAR and Lα·H_2O separately. PAR and Lα·H_2O were SD separately (n = 3) to investigate the tabletting behaviour of the two components individually. PAR solutions and Lα·H_2O suspensions were SD using the same conditions as described in Table 1 and Section 2.2.1.1 with the exemption of the concentration with both materials being processed at 5% w/v.

2.2.1.3. Preparation of physical mixtures. For comparison purposes, 1:1 w/w physical mixtures of unprocessed PAR and Lα·H_2O (PM non-SD) as well as PAR and Lα·H_2O, which where spray dried separately using conditions as outlined in Table 1 and Section 2.2.1.2, (PM SD), were made up. The mixtures were obtained by physically mixing both components together for 10 min using a spatula.

2.2.2. Characterisation of powders

2.2.2.1. Quantification of PAR and Lα•H_2O in spray dried deposits collected from glassware wall. PAR and Lα•H_2O quantification in the material deposited on the inner walls of the spray dryer drying chamber, drying chamber-cyclone connector and cyclone was performed to test the powder's homogeneity. Random samples were taken (n = 3) of the

Table 1
Summary of spray dryer experimental parameters. T_{out} – outlet temperature, $C_{s1,i}$ – concentration of EtOH used, $C_{s2,i}$ – concentration of H_2O used. N/A – not applicable.

Sample number	T_{out} (°C)	$C_{s1,i}$ (% v/v)	$C_{s2,i}$ (% v/v)	Excipient soluble fraction in mixture (%) (McDonagh and Tajber, 2020)
#1	86 ± 1	100	0	0.13 ± 0.18
#2	78 ± 1	90	10	0.81 ± 1.15
#3	75 ± 1	80	20	1.63 ± 2.31
#4	73 ± 1	70	30	6.54 ± 1.46
#5	72 ± 1	60	40	16.97 ± 1.91
#6	70 ± 1	50	50	45.89 ± 1.34
PAR SD	77 ± 1	100	0	N/A
Lα·H_2O SD	85 ± 1	100	0	N/A

deposited material from each region, accurately weighed using a microbalance (Mettler Toledo MT5, Switzerland), and then placed in 50 mL centrifuge conical tubes. 45 mL of EtOH was added to each tube, the vials were sealed well, and then shaken for one hour at a rate of 200 rpm using an orbital shaker (IKA MTS 2/4, Germany). All samples were then moved to an incubator set at 25 ± 3 °C and left for 12 h to give the suspension adequate time to settle to the bottom of the vial. The quantification of both components was then performed as previously described (McDonagh and Tajber, 2020).

2.2.2.2. Particle size analysis. Measurements of particle size and particle size distributions were obtained using a laser diffraction particle sizer (Mastersizer 3000, Malvern Instruments, U.K.) ($n = 3$). Particles were dispersed using a Malvern Aero S accessory equipped with a micro volume sample tray using 3 bar pressure. An obscuration of between 0.5 − 6% was obtained using a vibration feed rate of 75%. A pressure titration was conducted before measurements to ensure that the pressure applied did not induce particle breakage during testing. This was performed by measuring the particle size at various air pressures to determine at what pressure particle breakage and attrition occurred. Mastersizer 3000 software (v 3.63) was used for analysis and to generate the particle size distribution data of the dry powder samples.

2.2.2.3. True and tap density. The true density of the powders ($n = 3$) was determined using an AccuPyc 1330 pycnometer (Micromeritics, Norcross, GA, USA) using helium (99.995% purity). A 1 cm^3 cell was used, the equilibration rate was 5×10^{-3} psig/min and the system was purged 10 times. Tapped density ($n = 3$) was measured by adding a known quantity of material to a 5 mL graduated glass cylinder and tapping the cylinder off the table top the required number of times for the compacted powder to reach a constant volume value (Yang et al., 2012). Once the volume reading was constant over 100 tap periods, the weight was measured again and the density was calculated.

2.2.3. Tablet preparation

Tablets of 200 ± 2 mg weight were produced using a laboratory scale single punch NP-RD10 Manually Operated Tablet Press (Natoli Engineering Co Inc. USA). The die, lower punch and upper punch were lightly lubricated with magnesium stearate using a brush prior to compression. A minimal amount of lubrication was used as to not influence the tablet weight and/or mechanical strength. The powder was compressed at forces of 1250, 2500, 5000, 7500, 10,000, 12,500 and 15,000 N using 8 mm flat faced punches corresponding to compression pressures of 25, 50, 100, 149, 199, 249 and 299 MPa, respectively. The dwell time of each tablet under compression was approximately 1 min (Paczkowska et al., 2020). The tablets were accurately weighed using a microbalance (Mettler Toledo MT5, Switzerland) and inspected after the compression process for defects such as lamination, chipping, capping and sticking.

2.2.3.1. Heckel plots. The following model was proposed by Heckel (Heckel, 1961).

$$ln\left(\frac{1}{1-D}\right) = KP + A \tag{6}$$

where D is the relative density of the compact, P is the applied pressure, A is a constant suggested to represent particle rearrangement and the reciprocal of K is used to calculate apparent mean yield pressure (P_y). Heckel plots were produced for each compact investigated by plotting the natural log of 1/1-D versus the compaction pressure (MPa) used. The slope of the plot was taken from a point qualitatively chosen to be the centre of the most linear region of the curve and a linear regression fitting approach as described by Hooper et al. applied (Hooper et al., 2016). The linear region was extended in approximately 10 MPa steps. Once the part of the curve which contained the highest regression coefficient (specific to x coordinate) was established the step size was decreased until an accuracy of 1 MPa was reached (Hooper et al., 2016).

2.2.4. Mechanical properties of tablets

Dimensional analysis, tablet breaking force and the tablet weight was measured immediately after tablet ejection to reduce variance that could arise due to the tablets hygroscopicity or elastic recovery. All tests performed are detailed below.

2.2.4.1. Dimensional measurements. Dimensional analysis of the tablets was preformed using a 0 – 25 mm 1×10^{-3} mm digital micrometre (Digital Measurement Metrology, Toronto, Canada). Tablets were lightly de-dusted using a brush immediately after ejection and the compact's width and thickness were then measured carefully as to not crush or chip the tablet prior or tablet breaking force testing (Paczkowska et al., 2020).

2.2.4.2. Tablet tensile strength and porosity. The tablet breaking force was measured with a Digital Portable Hardness Tester EH-01 94,010, (Electrolab, India) from an average of 10 tablets. Tensile strength (σ) represents the resistance of the tablets to fracturing under diametric compression between two flat faces. Tensile strength values were calculated from the Breaking Force (F) values using Eq. (1) assuming conditions of ideal line loading (J. Fell and Newton, 1970; Akande et al., 1997), where d is the diameter of the tablet and h is the thickness of the tablets (J. Fell and Newton, 1970).

$$\sigma = \frac{2F}{\pi hd} \tag{1}$$

Eq. (1) can only be used when testing round, flat-faced tablets (Newton et al., 2000). Solid fraction (SF), was calculated using Eq. (2), where Wt is the tablet weight, v is volume of tablet and ρ_{true} is true density of the powder (Govedarica et al., 2009; Paczkowska et al., 2020; Iyer et al., 2014).

$$SF = \frac{Wt}{\rho_{true} \cdot v} \tag{2}$$

The tablet porosity (ε) was then calculated from SF using the following equation (Paczkowska et al., 2020; Iyer et al., 2014).

$$\varepsilon = 1 - SF \tag{3}$$

The compaction pressure was calculated from the applied compression force and the cross-sectional area of the tablets.

2.2.5. Friability testing

Friability tests were conducted using a Friability Tester Model TA 20 (Copley Scientific, UK). 10 tablets were dusted and accurately weighed before placing in the drum apparatus. Tablets were then tested for 4 min (100 rotations) before removing the tablets, re-dusting and re-weighing. This procedure was conducted for each of the compression pressures used. The criteria to pass the friability test was a weight loss of no more than 1% as per the USP (U.S.Pharmacopeia, Tablet friability, 2019).

2.2.6. Disintegration testing

Disintegration tests were conducted using the Erweka ZT 44 Tablet Disintegration Tester (Copley Scientific, UK). Six tablets were placed into each of the six glass tubes (one tablet per each tube) with open tops and mesh screens on the bottom. The basket racks containing the tubes with the tablets were submerged in 900 mL of deionised water at 37 ± 2 °C. These were oscillated up and down through a distance of 5 - 6 cm at 28–32 cycles per min. The time it took for all the tablets to disintegrate and for all of the particles to pass through the 10-mesh screen was recorded as the disintegration time. This procedure was conducted for each of the seven compression pressures investigated.

The criteria to pass the disintegration test was a disintegration time no longer than 15 min as per the USP (U.S.Pharmacopeia, Disintigration, 2019; British-Pharmacopoeia, Disintigration testing, 2019).

2.2.7. Dissolution testing and evaluation of dissolution profiles

Dissolution tests for PAR were conducted as per the USP monograph for acetaminophen tablets using a Vanderkamp 6 Spindle Dissolution Tester VK600 (Vankel Industries, USA) configured into a paddle apparatus (apparatus 2) using sink conditions (U.S.Pharmacopeia, Acetaminophen Tablets, 2019). Three tablets made at each compression force were selected and each tablet was then placed into a separate dissolution vessel containing 900 mL phosphate buffer (solution of monobasic potassium phosphate adjusted to pH 5.8 with NaOH) maintained at 37 °C (U.S.Pharmacopeia, Acetaminophen Tablets, 2019). The rotation speed of the paddles was 50 rpm. Tablets were added after the dissolution medium had reached a steady velocity and settled to the bottom of the bath once added. An aliquot of 5 mL from each bath was withdrawn using a syringe at each time point, filtered (25 mm syringe filter with a 0.45 µm polyethersulfone membrane, Fischer, Ireland), diluted and then tested using UV–Vis spectroscopy at a wavelength of 243 nm. Samples from the vessels were withdrawn at several time intervals; 1 min, 2 min, 5 min, 10 min, 20 min, 30 min, 40 min, 50 min and 60 min, and at 10 min intervals after this up to 120 min if 100% release had not been achieved by then. This procedure was conducted for tablets made at each of the seven compression forces of the 50/50% v/v EtOH/H_2O (#6) and PM non-SD samples.

Dissolution profiles were evaluated by calculating the f_1 and f_2 fit factors for every pair of dissolution curves obtained from tablets made at a given compression pressure (Moore and Flanner, 1996), taking that of the tablets made of the physical mixture (PAR and Lα•H_2O 50:50 w/w, unprocessed) as the reference (R) and that of the CC-SD powder (#6) as the test sample (T). In brief, the difference factor (f_1) measures the dissimilarity between two dissolution profiles at different time points, while the similarity factor (f_2) calculated the degree of closeness between two dissolution curves. The f_1 and f_2 values were calculated using Eqn. (4) and Eqn. (5) using DDSolver, an Excel add-in for modelling and comparison of drug dissolution profiles (Zhang et al., 2010):

$$f_1 = \left\{ \frac{\sum_{t=1}^{n} |R_t - T_t|}{\sum_{t=1}^{n} R_t} \right\} \cdot 100 \quad (4)$$

$$f_2 = 50 \cdot \log\left\{ \left[1 + \frac{1}{n} \sum_{t=1}^{n} (R_t - T_t)^2 \right]^{-0.5} \cdot 100 \right\} \quad (5)$$

where n is the number of timepoints, R_t and T_t are the mean percent dissolved from the reference and test products at a timepoint t, respectively. The f_1 value is equal to 0 and the f_2 factor is 100 when the R and T dissolution profiles are the same (Moore and Flanner, 1996).

3. Results and discussion

3.1. Evaluation of powders and mechanical properties of tablets

As previously described, all CC-SD PAR and Lα·H_2O samples were crystalline post spray drying with no polymorphic change in either the PAR or the Lα·H_2O seen (McDonagh and Tajber, 2020; McDonagh and Tajber, 2019). Also, the PAR and Lα·H_2O solubility in the hydro-ethanolic feed had a substantial influence on the morphology of the CC-SD agglomerates. A low excipient soluble fraction, when 100% ethanol was used, produced an increase in PAR surface coating and a high excipient soluble fraction, when ethanol/water 1:1 v/v mixture was used, resulted in agglomerates of highly mixed components (Fig. 1) (McDonagh and Tajber, 2020). It was therefore anticipated that the variability in the degree of intimate mixing following a crystallo-co-spray drying process may affect the downstream processing, in particular tabletting, of the materials obtained.

The median particle size of the CC-SD materials varied between 13.6 µm (sample #1) and 16.4 µm (sample #4) (McDonagh and Tajber, 2020) and the particle size data for the other samples are presented in Table 2. Table SI.1 gives the number of tablets produced and the number tested for each material at each compression pressure. What is also given is the number of tablets produced that showed signs of lamination; these tablets were not further tested. Lamination is the splitting of a tablet into two or more distinct horizontal layers. Similar to capping, the cause of this is as a result of entrapped air during the compression process or if the material tabletted exhibits elastic recovery (Khan and Rhodes, 1973). Most of the CC-SD materials showed a lower tendency to laminate in comparison to the physically mixed materials with no tablet defects seen at any compression pressure for samples #3 - #6. For materials CC-SD at higher EtOH concentrations such as samples #1 and #2, defects did occur at higher compression pressures due to the effect of over compaction and increasing tendency for elastic recovery (Fig. 2). The robustness of the crystallo-co-spray drying process is highlighted in the instability of the individual components and physical mixtures during the tabletting process (Fig. 2). The PM SD, PM non-SD, PAR SD and PAR non-SD all showed increased signs of lamination at lower compression pressures in comparison to the CC-SD samples. No tablets could be produced for both PAR materials (SD and non-SD) as well as the PM non-SD, at the highest compression pressure tested (299 MPa) due to the high lamination tendency.

3.1.1. Compressibility

Fig. 3 shows the compressibility profiles of the various tablet samples. With an increase in compression pressure, the sharpest decrease in porosity was attributed to the #6 sample. The next sharpest decrease was seen in the #5 sample with all other CC-SD samples behaving similarly with the exception to the #1 sample which reduced in porosity to the smallest extent. The largest decrease in volume was associated with the #6 sample. Under compression a powder reduces in volume until reduction is no longer possible and deformation occurs. A larger reduction in volume results in the shortening of the distance between particles and therefore an increase in interparticle bonding. With this increase in bonding area comes an increase in compact strength as seen in Fig. 2.

The large reduction in material porosity for the #6 sample seen in Fig. 3 was due to the material's low tap density (Table 2). At higher water concentrations more Lα•H_2O was SD from solution resulting in a greater degree of intimate mixing in the final dried agglomerate (McDonagh and Tajber, 2020). With this increase in mixing came a decrease in material tap density in comparison to at higher EtOH concentrations in which Lα•H_2O was predominantly SD from suspension. With the #6 agglomerate having the lowest tap density, an increase in compression pressure lead to the largest reduction in porosity (Fig. 3). The largest decrease in volume on tapping of the physical mixtures and individual components of the agglomerates was attributed to the PAR SD. It was the most porous material of the physical mixtures and individual components, which could be a result of it being the only material SD from solution. In work previously described, PAR was SD from solution and characterised based on the physical characteristics of atomised droplets. It was found that spray drying from solution had the effect of forming semi-spherical particles of varying densities based on the spray drying parameters chosen (McDonagh and Tajber, 2019). This can also be seen in Table 2 with the lowest tap density value of the individual components being attributed to the PAR SD material.

All SD materials had lower tap density in comparison to their non-SD counterparts (Table 2). This resulted in larger reduction in material porosity values for the SD materials as the compression pressure increased (Fig. 3). Similar to the above, with a greater reduction in material porosity and subsequent increase in interparticle interaction, there was an increase in compact tensile strength (McKenna and McCafferty, 1982). For this reason, there was an increase in tensile

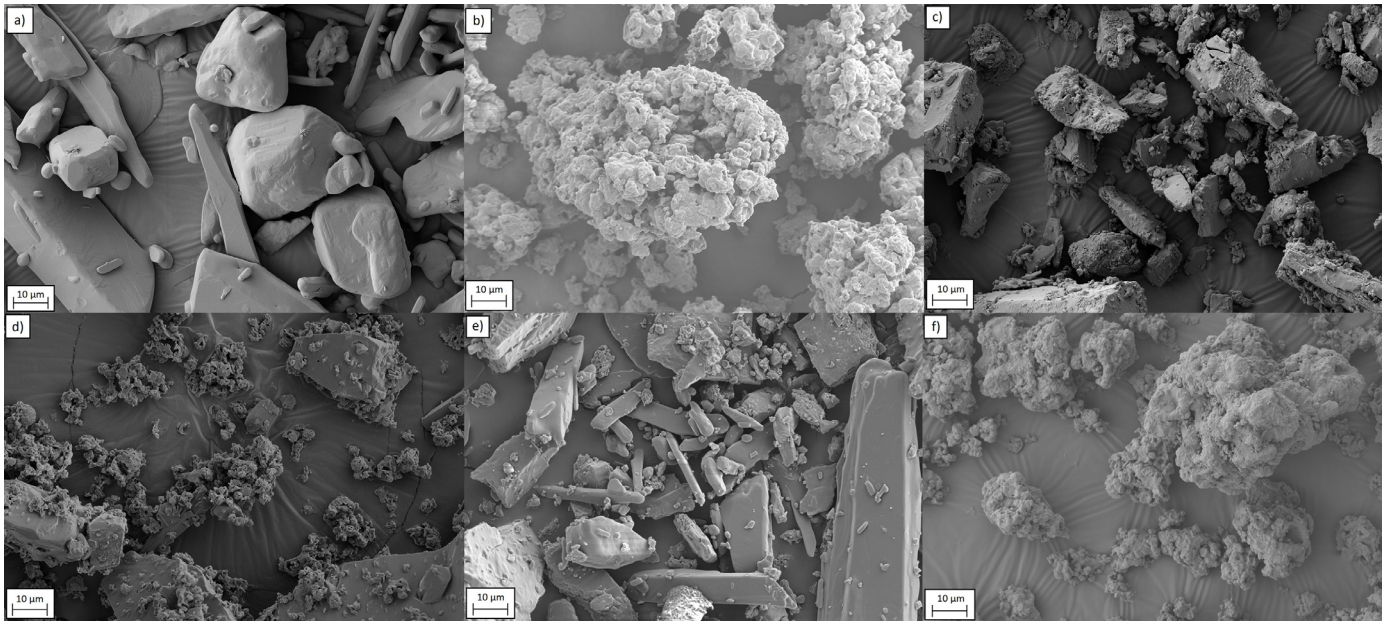

Fig. 1. Scanning electron microscopy images of PAR as received from the supplier (PAR non-SD, a), PAR spray dried using 100% EtOH (PAR SD, b), Lα•H_2O as received from the supplier (LAC non-SD, c), Lα•H_2O spray dried using 100% EtOH (Lα•H_2O SD, d), PAR + Lα•H_2O physically mixed 1:1 ratio (PM non-SD, e) and PAR + Lα•H_2O spray dried separately and then physically mixed (PM SD, f).

Table 2
True density, tap density, particle size distribution and mean yield pressure (P_y) of the samples tested.

Sample number	True density (g/cm^3)	Tap density (g/cm^3)	Particle size distribution*			P_y (MPa)
			d(0.1) µm	d(0.5) µm	d(0.9) µm	
#1	1.38 ± 0.02	0.654 ± 0.017	3.24 ± 0.44	13.60 ± 0.73	53.39 ± 6.34	166.6
#2	1.39 ± 0.01	0.638 ± 0.018	3.45 ± 0.56	15.79 ± 1.28	64.09 ± 6.28	153.8
#3	1.39 ± 0.01	0.618 ± 0.019	3.71 ± 0.33	16.37 ± 1.00	68.45 ± 6.79	151.5
#4	1.40 ± 0.01	0.593 ± 0.017	3.84 ± 0.30	16.39 ± 0.28	64.82 ± 5.27	135.1
#5	1.39 ± 0.01	0.564 ± 0.024	3.79 ± 0.55	16.01 ± 0.84	51.70 ± 7.56	131.6
#6	1.36 ± 0.01	0.548 ± 0.014	3.89 ± 0.25	14.38 ± 0.49	38.91 ± 1.46	93.4
PM SD	1.46 ± 0.01	0.598 ± 0.009	5.42 ± 0.25	29.50 ± 0.61	117 ± 5.79	294.1
PM non-SD	1.42 ± 0.01	0.773 ± 0.006	5.09 ± 0.05	21.80 ± 0.33	83.05 ± 7.11	714.3
PAR SD	1.31 ± 0.01	0.549 ± 0.011	2.33 ± 0.16	11.36 ± 0.84	24.44 ± 1.46	138.8
PAR non-SD	1.32 ± 0.01	0.684 ± 0.009	1.86 ± 0.11	7.82 ± 0.24	17.13 ± 0.38	256.4
Lα•H_2O SD	1.50 ± 0.01	0.726 ± 0.022	3.88 ± 0.17	25.21 ± 0.21	86.81 ± 1.42	136.9
Lα•H_2O non-SD	1.48 ± 0.03	0.806 ± 0.006	4.42 ± 0.09	25.04 ± 0.70	88.41 ± 2.85	212.7

* - data for the systems #1-#6, PM non-SD and Lα•H_2O non-SD were reprinted from (McDonagh and Tajber, 2020), with permission from Elsevier.

strength for materials that were SD in comparison to their non-SD counterparts (Fig. 2). Both Lα•H_2O materials had the highest tablet bulk density accounting for the low porosity seen in Fig. 3. This is evident in materials that undergo brittle fragmentation under compression leading to an increase in densification (Vromans et al., 1985).

To help understand the densification process further, Heckel plots were derived for each compact tested (Fig. 4). Fig. 4a shows the Heckel plots of the CC-SD agglomerates. During the initial stages of compression, the #6 agglomerate underwent more extensive densification in comparison to the other agglomerates. This may be due to the #6 agglomerates readily undergoing more rearrangement at low compression pressures due to the low density of the particles (Table 2). Further rearrangement and densification were also facilitated by the fragmentation of the Lα•H_2O constituent of the agglomerate in which the #6 agglomerate had the highest degree of PAR - Lα•H_2O interaction. Towards the higher end of the compression pressures used the #6 agglomerate exhibited plastic behaviour however, its densification appeared to be hindered indicating a maximum compression had been reached. The other agglomerates exhibited a much more gradual densification process in comparison. Fig. 4b gives the Heckel plots of the individual components of the CC-SD agglomerates investigated. Similar to the #6 agglomerate, the SD samples exhibited a more extensive densification process in comparison to their non-SD counterparts also in line with the trends seen in the tap density values (Table 2). The LAC SD sample underwent the largest degree of densification and the PAR non-SD sample underwent the least, in line with the material's poor compressibility evident in signs of overcompaction. The mean yield pressure values (Table 2) indicate that the #6 agglomerate, with the lowest P_y value, exhibited the most plastic behaviour in comparison to other systems.

3.1.2. Compactibility

The tabletability profiles of PAR and Lα•H_2O CC-SD agglomerates at various inlet feed solvent compositions can be seen in Fig. 2 and of the individual components of the agglomerates both SD and non-SD, together with their physical mixtures, in Fig. 2. The #6 agglomerate produced tablets with the highest tensile strength at the lowest compression pressures used. As the compression pressure increased, using this sample, past a maximum tensile strength achieved at 100 MPa, the strength of the tablets decreased as a result of overcompaction. At this maximum, the #6 sample had a tensile strength 1.5 times larger than the #5 sample and 2.9 times the strength of the PM SD. The #5 sample

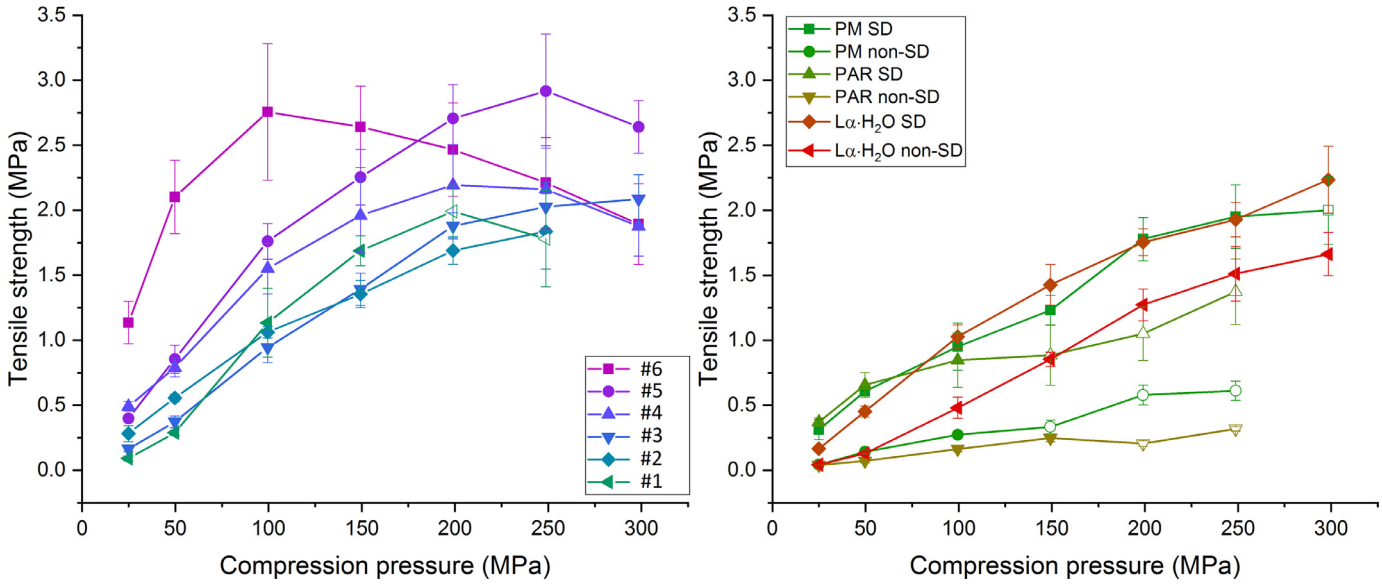

Fig. 2. Tabletability profiles of PAR and Lα·H_2O mixtures CC-SD at various inlet feed solvent compositions and their individual components both SD and non-SD as well as their SD and non-SD physical mixtures. A solid datapoint indicates that all tablets produced were free from any defects, a hollow datapoint indicates that some tablets showed defects (Table SI.1) and if no datapoint is present then no tablets could be reliably produced at that compression pressure. Lines are to guide between datapoints only. Error bars represent standard deviation.

had the highest tensile strength at a higher compression pressure reaching a maximum strength at 249 MPa with a similar trend in overcompaction seen as the compression pressure increased past this point. The average tensile strength of the compacts decreased with an increasing concentration of EtOH in the feed with the exception of the #1 sample that showed an improved strength over the #2 and #3 samples over the compression pressures of 100 MPa, 149 MPa and 199 MPa, however tablets could not consistently be produced at the maximum compression pressure used of 299 MPa for the #1 sample due to the presence of lamination.

The compactibility of a material is its ability to be transformed into tablets of required strength during densification (Sun and Grant, 2001; Tye et al., 2005). This plot is quite useful for tablet evaluation as it represents two very important parameters, the tensile strength and porosity. Both may influence the dissolution properties of the compact. The compactibility profiles for both the CC-SD agglomerates and their individual components can be seen in Fig. 5.

It is favourable for a tablet to have an adequate tensile strength whilst maintaining a desired level of porosity (Tye et al., 2005). If such a trade-off can be achieved, then a tablet can be produced with a favourable mechanical strength and dissolution profile (Bandari et al., 2008). The #6 sample had the highest tensile strength on average with respect to the porosity. With an increase in the EtOH concentration of the CC-SD feed, the compactibility of the materials decreased up to a composition of 70% v/v EtOH/H_2O (#4) after which the so-SD mixtures behaved similarly. It can be seen in Fig. 5 that by spray drying the

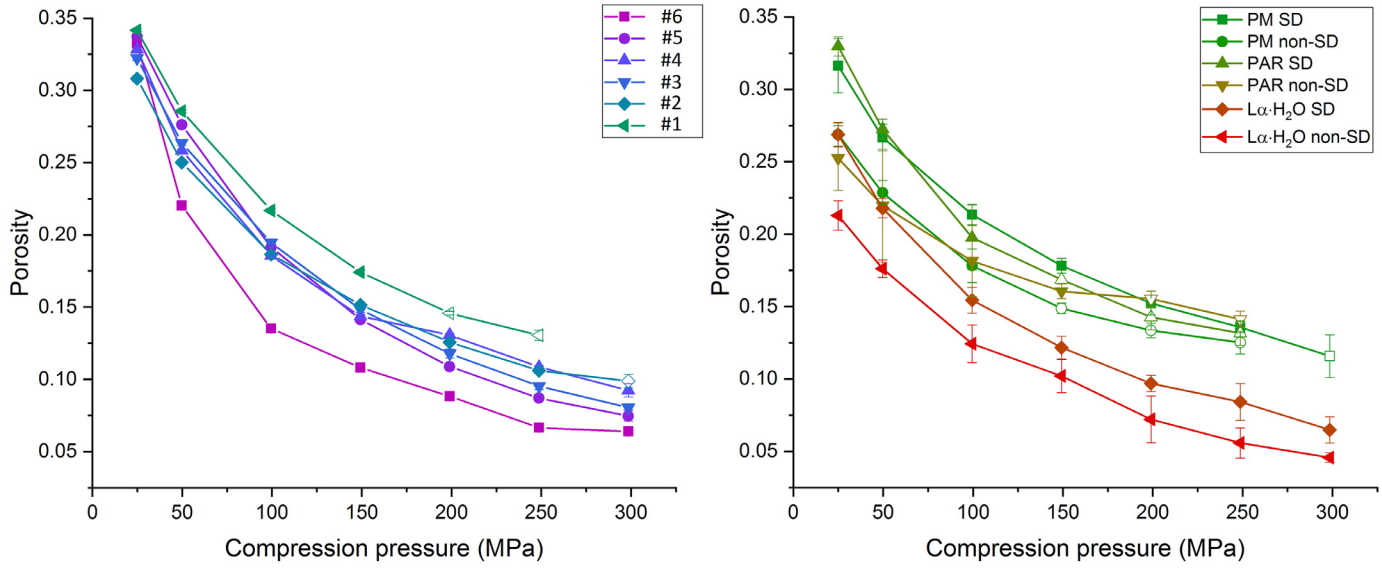

Fig. 3. Compressibility profiles of PAR and Lα·H_2O mixtures CC-SD at various inlet feed solvent compositions and their individual components both SD and non-SD as well as their SD and non-SD physical mixtures. A solid datapoint indicates that all tablets produced were free from any defects, a hollow datapoint indicates that some tablets showed defects (Table SI.1) and if no datapoint is present then no tablets could be reliably produced at that compression pressure. Lines are to guide between datapoints only. Error bars represent standard deviation.

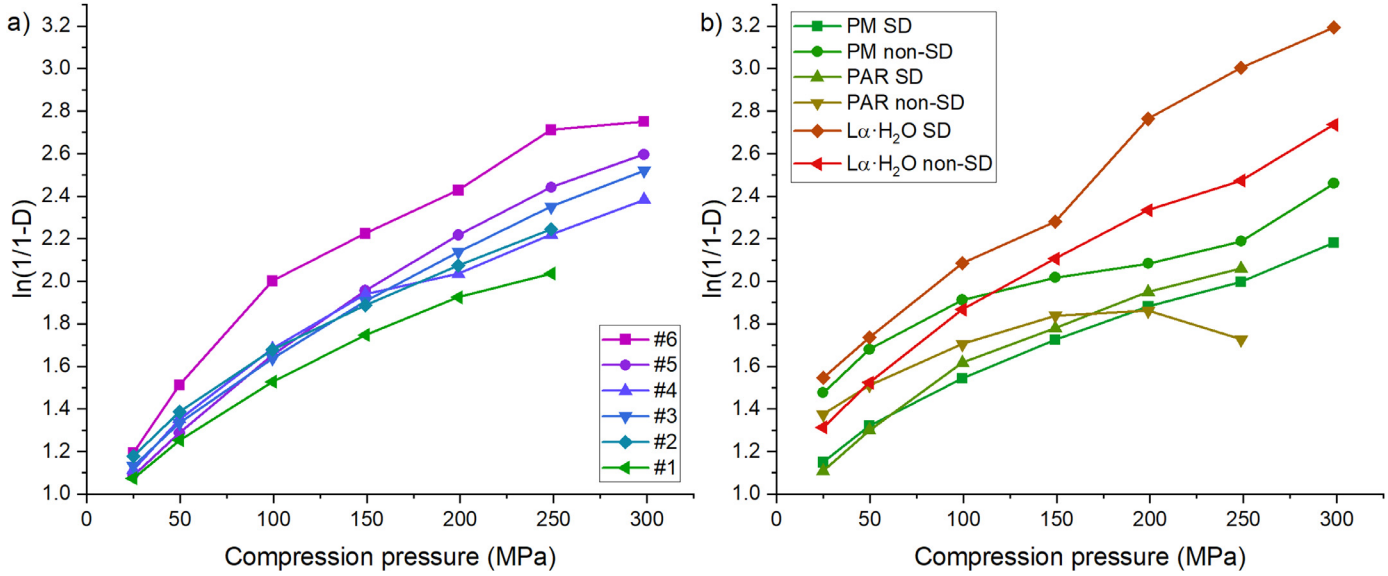

Fig. 4. Heckel plots for PAR + Lα•H_2O CC-SD mixtures (a) and the individual components (b) investigated.

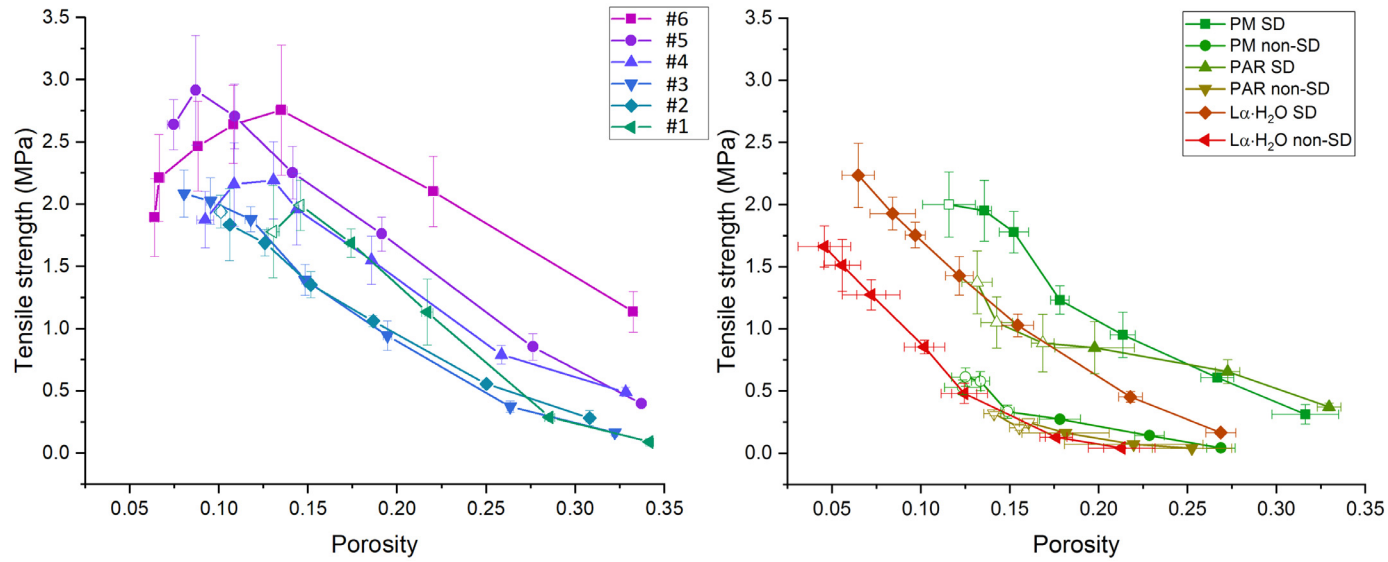

Fig. 5. Compactibility profiles of PAR and Lα•H_2O mixtures CC-SD at various inlet feed solvent compositions and their individual components both SD and non-SD as well as their SD and non-SD physical mixtures. A solid datapoint indicates that all tablets produced were free from any defects, a hollow datapoint indicates that some tablets showed defects (Table SI.1) and if no datapoint is present then no tablets could be reliably produced at that compression pressure. Lines are to guide between datapoints only. Error bars represent standard deviation.

individual components of the agglomerates, an improvement can be made to the compactibility profile with all SD materials behaving more favourably in comparison to their non-SD counterparts. The PM SD sample had the best compactibility profile of the individual components and physical mixtures in terms of maximising both tensile strength and porosity. The poor tabletting performance of PAR non-SD is evident in Fig. 5 in which all tablets produced had a low tensile strength as well as a high solid fraction indicating how unfavourable the material's crystal packing is for compaction.

Alderborn and Frenning state that the compactibility of a material is defined as the ability of a powder to form a coherent tablet as a result of compression, with such a material having a high resistance towards fracturing without tendencies to cap or laminate (Augsburger and Hoag, 2008). As evident in Fig. 2, the PM both SD and non-SD showed signs of such tablet defects at higher compression pressures. PAR SD and non-SD also showed signs of lamination and capping, which is common for the material (Garr and Rubinstein, 1991), resulting in no tablets being reliably produced at the maximum compression pressure investigated (299 MPa). But these defects were also present in the CC-SD agglomerates SD using 100% EtOH (#1) and 90% v/v EtOH/H_2O (#2) in the inlet feed with no tablets able to be produced for the #1 sample at this maximum pressure (Fig. 2). This is further evidence for the high compactibility of the CC-SD agglomerates processed at higher water concentrations/soluble fractions of the excipient in the spray dryer inlet feed (McDonagh and Tajber, 2020).

3.1.2.1. PAR and Lα•H_{2O} soluble fraction in inlet feeds. PAR was taken as the model drug in this study due to its poor compaction behaviour with tablet tensile strength only ranging from 0.04 MPa to 0.31 MPa (for compaction pressures of 25 MPa to 299 MPa respectively) (Fig. 2). In order to understand the improvement in tabletting performance associated with the crystallo-co-spray drying of PAR and Lα•H_2O we must first look at the soluble fraction of each component in the solvent feed. As presented previously (McDonagh and Tajber, 2020), by

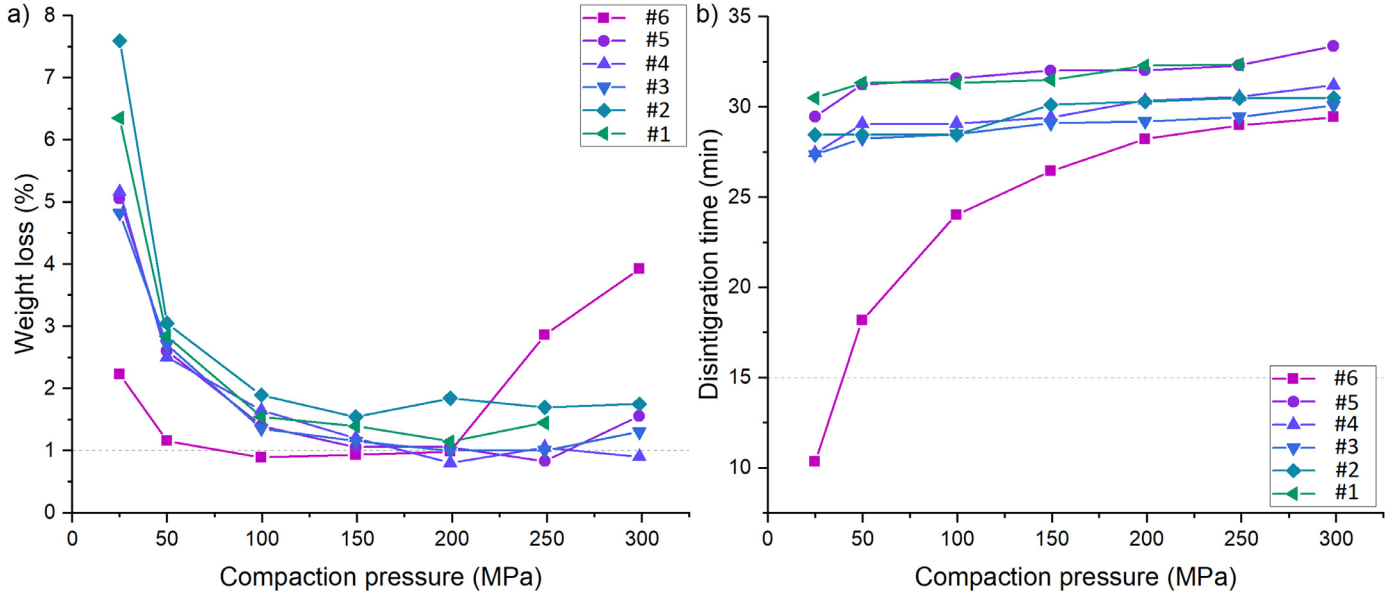

Fig. 6. Friability (a) and disintegration (b) profiles of tablets made of PAR + Lα•H_2O CC-SD mixtures. For friability testing, a weight loss < 1% is a pass (U.S.Pharmacopeia, Tablet friability, 2019) and for disintegration testing, a disintegration time < 15 min for uncoated immediate release tablets is a pass (U.S.Pharmacopeia, Disintigration, 2019). Solid lines are to guide between datapoints only. Dashed lines represent the criteria for passing.

crystallo-co-spray drying PAR and Lα•H_2O from a *Sc* of 50/50% v/v EtOH/H_2O (#6), 45.89 ± 1.34% of the Lα•H_2O was in solution together with 96.95 ± 0.22% of PAR. As an atomised droplet dried, both these components in solution precipitated almost simultaneously. This produced a dried particle consisting of highly mixed components. For the #1 sample, only 0.18 ± 0.13% of the Lα•H_2O was in solution as well as 96.72 ± 0.93% of the PAR. Due to the vast majority of Lα•H_2O now being in suspension, the only places that the precipitating PAR can form is either homogeneously in the bulk of the droplet or on the surface of the suspended Lα•H_2O particles, greatly reducing the degree of intimate mixing in the final dried powder blend. With an increase in soluble fraction of Lα•H_2O in the solvent feed also came a minor decrease in Lα•H_2O crystallinity in the final spray dried agglomerate, as evidenced by powder X-ray diffraction and dynamic vapour sorption (McDonagh and Tajber, 2020). This increase in disorder may have impacted on particle rearrangement under compression resulting in an improvement in the tabletability of the material evident in Fig. 2 in which Lα•H_2O that was spray dried showed an improvement over its non-SD counterpart. For these reasons, the #6 sample showed a greater improvement in tabletability at low compression pressures compared to agglomerates produced by crystallo-co-spray drying from higher EtOH feed concentrations. The improvement over the PM SD shows that a stronger tablet is obtained when both components are SD simultaneously in comparison to individually and then physically mixed.

Tablet compaction increases strength through particle fracture and packing rearrangement where the bed is sheared and the particles are deformed (Hiestand, 1997). As stated by Hoag et al., through the process of compaction, the volume between particles is reduced and rearrangement occurs into a closer packing structure. At some point, the packing characteristics of the powder and friction between the particles prevent any further reduction in volume and at this point the particles deform either elastically (reversible), plastically (irreversible) or viscoelastically (Hoag et al., 2008). Some materials fragment under compression such as Lα•H_2O, which further reduces the powder volume (Vromans et al., 1985). As a result of this process, particle surfaces come into close proximity leading to the formation of interparticle bonds and therefore increasing compact strength (Hoag et al., 2008). Chadwick et al. and Telford et al. found molecular functionality between the hydroxyl groups of the Lα•H_2O molecule and the hydroxyl and amide groups of the PAR form I molecule (Chadwick et al., 2012; Telford et al., 2016). In work previously published by this research group, second derivative Fourier transform infra-red spectroscopy analysis of CC-SD PAR and Lα•H_2O showed subtle changes in these functional groups in both materials (McDonagh and Tajber, 2020). With an increase in soluble fraction of the excipient in the spray dryer inlet feed, there was a higher degree of intimate mixing in the final dried agglomerate (McDonagh and Tajber, 2020). During consolidation, this increase in drug-excipient mixing increased the interparticle bonding strength and therefore the tensile strength of the resulting compact (Fig. 2). With a reduction in component mixing, this strength decreased, evident in materials CC-SD at higher EtOH concentrations. Also, considering similar tap density values (Table 2), the #6 sample had the largest tensile strength indicating that at the same material compaction, this sample had the strongest interparticle bonding.

At a compression pressure of 149 MPa, a third of tablets produced from the physically mixed blend of PAR + Lα•H_2O (PM non-SD) showed signs of lamination as a result of the poor compressibility of the material further emphasising the improvement associated with spray drying. Lα•H_2O SD showed an improvement in tabletability in comparison to its non-SD counterpart. A similar trend was seen for PAR with the PAR SD having a greater tensile strength at each compression pressure compared to PAR non-SD. At the final compression pressure used of 299 MPa, there was no data point for either the PAR SD or the PAR non-SD due to tablet capping and lamination, as evident in materials prone to elastic deformation (Garr and Rubinstein, 1991; Di Martino et al., 1996). The improvement in tabletability for SD materials over non-SD materials is down to the materials density which will be discussed in the next section.

3.2. Functional properties of tablets

3.2.1. Friability and disintegration

To further emphasise the effect of component soluble fraction on the improvement in physiochemical properties associated with the crystallo-co-spray drying of PAR and Lα•H_2O, friability and disintegration studies of the tablets were also conducted (Fig. 6).

The #6, #5 and #4 agglomerates all compressed into tablets that obtained the required maximum% weight loss of 1% to pass friability testing (Fig. 6a). The #6 tablets produced at 100 MPa, 149 MPa and

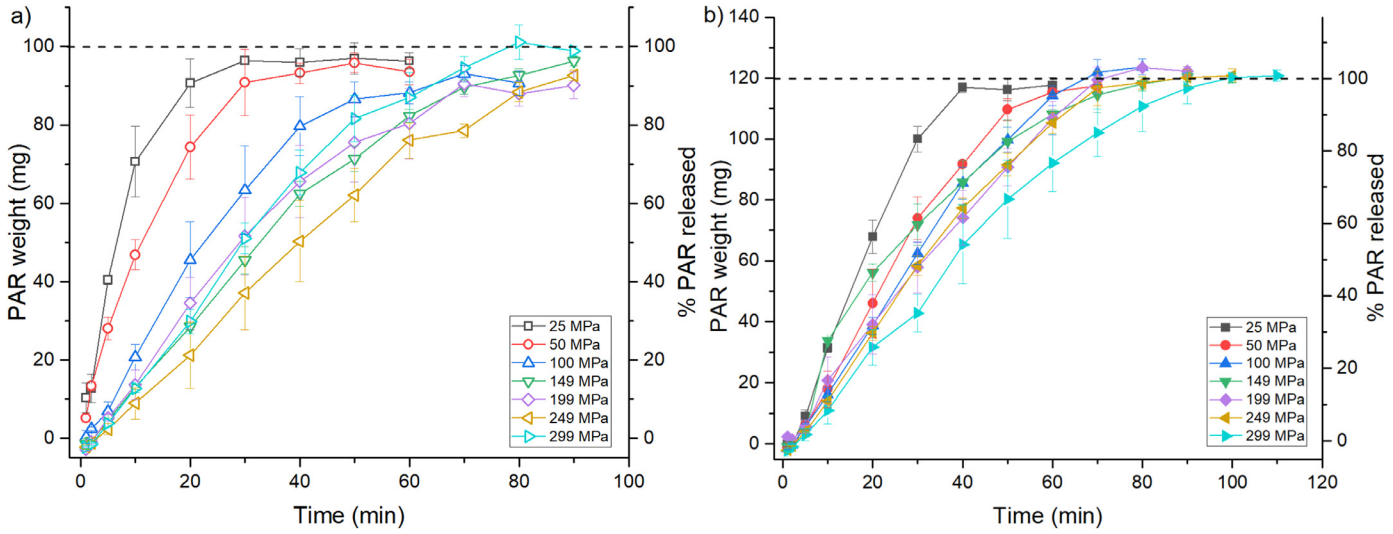

Fig. 7. Dissolution profiles of tablets made of: a) the physically mixed PAR + Lα•H_2O sample that was not spray dried (PM non-SD and b) CC-SD #6 sample at various compression pressures showing the weight and percentage of PAR released over time. Total tablet weight was 200 mg, the broken lines indicate the drug loading. Error bars represent standard deviation.

199 MPa all passed this criterion. The effect of over compaction of the #6 sample is evident in Fig. 6a with a sharp increase in% weight loss for tablets produced at the maximum compression pressure. Interestingly, the #6 sample behaved differently to the rest of the other CC-SD mixtures with respect to the disintegration tests. All tablets made of CC-SD samples disintegrated between 27 and 32 min however the tablets prepared at the lowest compression pressure used of 25 MPa disintegrated as quickly as 10.6 min, satisfying the maximum allowable time of 15 min for uncoated tablets to disintegrate according to the British Pharmacopeia (British-Pharmacopoeia, Disintigration testing, 2019).

3.2.2. Dissolution studies

The dissolution profiles of the tablets made of CC-SD #6 sample and of the physically mixed PAR + Lα•H_2O sample that was not spray dried (PM non-SD), at various compression pressures can be seen in Fig. 7. The tablets made of the physically mixed sample released the drug quicker than the tablets made of the CC-SD sample as a result of the tablet's inferior compaction (Fig. 7a). The #6 agglomerate produced much harder tablets in comparison to the PM non-SD which is evident in Fig. 2.

The f_1 and f_2 values calculated using Eqns. (4) and 5 show that the dissolution profiles of the tablets made of the CC-SD powder and of the physically mixed PAR + Lα•H_2O were different when 25, 50 and 299 MPa compression pressure was used (Table 3). Considering both fit factors, only the tablets compacted at 199 MPa can be regarded as comparable, since the value of f_1 was below 15 and the f_2 value was above 50 (Moore and Flanner, 1996). However, the formulations tabletted at 100, 149 and 249 MPa may also be considered as similar, based on one fit factor only, f_2 (Table 3).

Table 3
The f_1 and f_2 values for the dissolution profiles of tablets made of PAR and Lα•H_2O (50:50 w/w). The dissolution curves obtained from tablets by compacting the physical mixture of unprocessed components were taken as the reference product (R), while the dissolution curves of the tablets made of the CC-SD powder were taken as the test product (T). Values in large bold italic font indicate similar profiles ($f_1 < 15$ and/or $f_2 > 50$).

Compaction pressure (MPa)	f_1	f_2
25	27.27	30.21
50	32.48	30.99
100	16.21	51.95
149	16.29	52.08
199	9.40	69.06
249	18.97	56.80
299	22.45	46.88

What was interesting was that the tablets of the CC-SD material (#6) dissolved giving a higher PAR concentration, equivalent to around 120 mg drug loading, than expected and not consistent with the PAR to Lα•H_2O ratio of 50/50% w/w. Analysis of wall deposition in the spray dryer for the #6 agglomerate found that around 88% w/w of material deposited on the inner wall of the drying chamber was Lα•H_2O as was 48% of material in the drying chamber-cyclone connector and 38.5% of material deposited in the cyclone. With more Lα•H_2O being deposited on the inner walls of the dryer then PAR, there was a greater concentration of PAR in the final dried particle blend with an average drug content of 58.5 ± 2.6% w/w in the final powder blend. This makes the results previously described even more significant in that a stronger tablet compact is produced in comparison to physical mixtures even with a higher concentration of PAR with its inherent poor tabletting properties being present.

3.3. Tablet profiles summary

A summary of the CC-SD sample's tablet characterisation (tabletability, compressibility and compactibility (Tye et al., 2005)) is given in Fig. 8 below. The desirable characteristics of a tablet compact in which the strongest tablet possible is produced at the lowest compression pressure required while also maintaining the highest material porosity is best described in Fig. 8f for the #6 sample. For this CC-SD material, a compression pressure of 100 MPa best fits the above criteria. Tabletability (Fig. 2), compactibility (Fig. 5) and compressibility profiles (Fig. 3) indicate that the #6 sample exhibits the best physical properties for direct compression in comparison to agglomerates SD using higher EtOH concentrations in the spray dryer inlet feed and compared to the individual components of the agglomerates both SD and non-SD. It was the best performing sample with a decrease in processability from here as the concentration of EtOH increased in the spray dryer inlet feed (#5 - #1).

Tabletability profiles show that stronger tablets are produced with an increase in component mixing of CC-SD PAR + Lα•H_2O agglomerates as a result of an increase in the water concentration of the spray dryer inlet feed (Fig. 2 and Fig. 7). Compactibility profiles showed that agglomerates CC-SD using higher soluble fraction of components in the inlet feed produced compacts with the highest tensile strength with

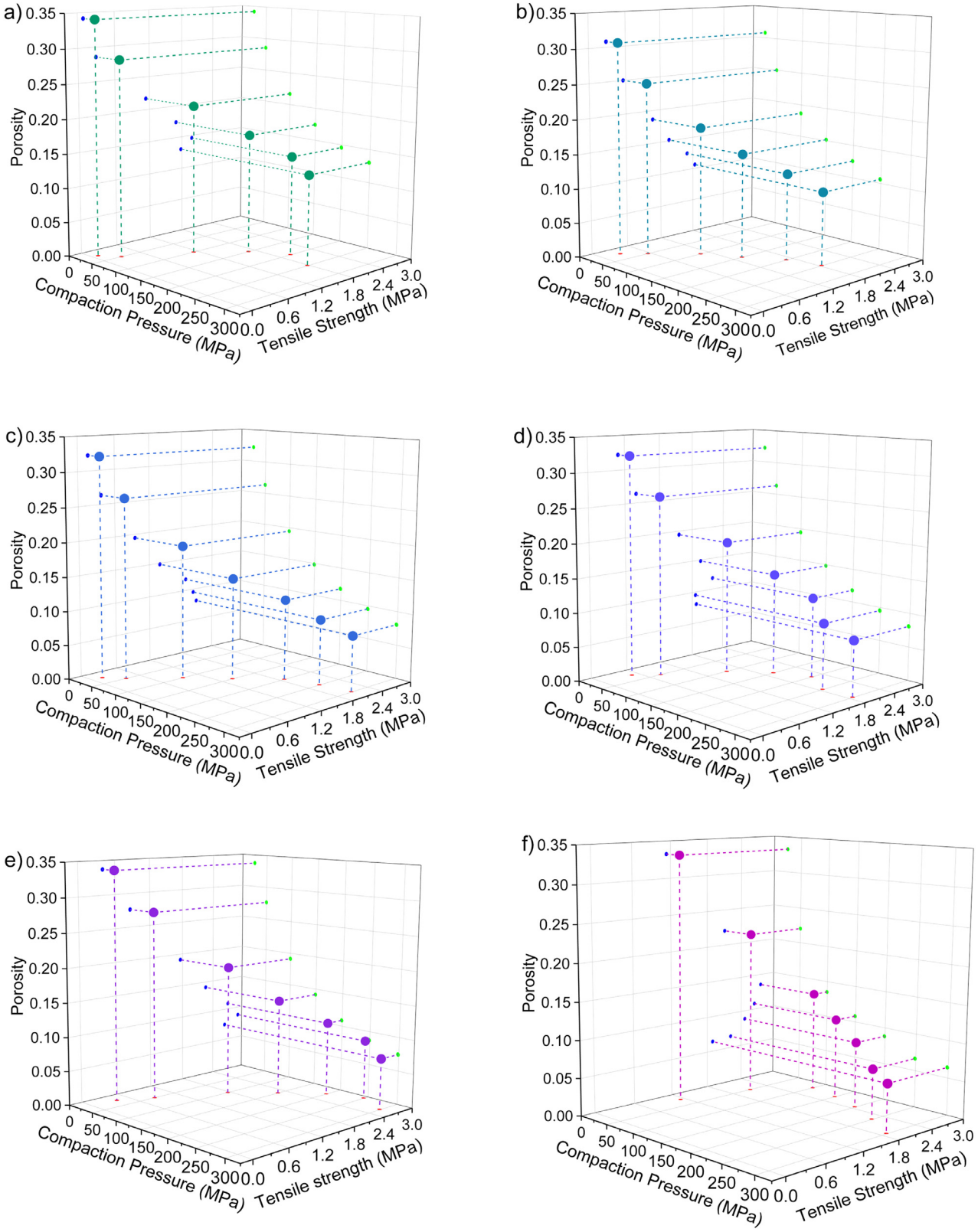

Fig. 8. 3D surface plots of tablet characterisation for PAR + Lα•H_2O CC-SD agglomerates SD using inlet feed solvent compositions: a) #1, b) #2, c) #3, d) #4, e) #5 and f) #6.

respect to the tablet's porosity (Fig. 5) and that at such soluble fractions, a material less prone to tablet defects such as lamination was produced. Compressibility profiles (Fig. 3) showed that this increase in tablet tensile strength was due to the increased volume loss associated with powders of lower tap density (Table 2), and an increase in inter-particulate bonding between PAR and Lα•H_2O molecules. The process of CC-SD enhances the masking ability of the excipient as stronger tablets are produced at lower compaction pressures even with an increase

in drug concentration in the powder blend (Fig. 2 and Fig. 7).

4. Conclusions

The crystallo-co-spray drying of a poorly compressible drug with a compressible excipient material can improve the tabletting performance of the agglomerate, through the process of crystallo-co spray drying, if the composition of the spray dryer inlet feed is properly evaluated. The increase in the degree of intimate mixing in the final spray dried agglomerate as a result of the increase in soluble fraction of the excipient in the spray dryer inlet feed as well as a slight increase in Lα•H_2O disorder, leads to improvements to the blend's tensile strength resulting in a tablet of higher mechanical strength being produced at lower compaction pressures even at higher drug ratios. Improvements to the tabletting properties of the individual components was also seen after spray drying with both PAR and Lα·H_2O forming harder compacts after spray drying individually. With the increase in mechanical strength for the tabletted CC-SD agglomerates, the criteria to pass friability and disintegration testing could then be met. Therefore, the crystallo-co-spray drying of a drug and an excipient to improve the degree of intimate mixing can be used as a method to improve the tabletting properties of a blend to allow for direct compression to be utilised.

CRediT authorship contribution statement

Alan F. McDonagh: Conceptualization, Methodology, Formal analysis, Investigation, Writing - original draft, Visualization. **Bronagh Duff:** Methodology, Formal analysis, Investigation. **Lorna Brennan:** Formal analysis, Investigation. **Lidia Tajber:** Conceptualization, Writing - review & editing, Visualization, Supervision, Funding acquisition.

Acknowledgements

Research leading to these results was supported by the Synthesis and Solid State Pharmaceutical Centre (SSPC), financed by a research grant from Science Foundation Ireland (SFI) and co-funded under the European Regional Development Fund (Grant Number 12/RC/2275).

Supplementary materials

Supplementary material associated with this article can be found, in the online version, at doi:10.1016/j.ejps.2020.105505.

References

Ahmed, H., Shimpi, M.R., Velaga, S.P., 2017. Relationship between mechanical properties and crystal structure in cocrystals and salt of paracetamol. Drug Dev Ind Pharm 43, 89–97.
Akande, O.F., Rubinstein, M.H., Rowe, P.H., Ford, J.L., 1997. Effect of compression speeds on the compaction properties of a 1: 1 paracetamol–microcrystalline cellulose mixture prepared by single compression and by combinations of pre-compression and main-compression. Int J Pharm 157, 127–136.
Al-Zoubi, N., Odeh, F., Nikolakakis, L., 2017. Co-spray drying of metformin hydrochloride with polymers to improve compaction behavior. Powder Technol 307, 163–174.
Augsburger, L.L., Hoag, S.W., 2008. Mechanical strength of tablets. In: Alderborn, G., Frenning, G. (Eds.), Pharmaceutical Dosage forms: Tablets. Informa healthcare USA, New York, pp. 207–236.
Aulton, M.E., Taylor, K.M., 2017. Aulton's Pharmaceutics E-Book: The Design and Manufacture of Medicines. Elsevier Health Sciences.
Bandari, S., Mittapalli, R.K., Gannu, R., 2008. Orodispersible tablets: an overview. Asian J Pharm. 2, 2–11.
Broadhead, J., Edmond Rouan, S.K., Rhodes, C.T., 1992. The spray drying of pharmaceuticals. Drug Dev Ind Pharm 18, 1169–1206.
U.S.Pharmacopeia, Disintigration, 2019. In: Brown, W.E. (Ed.), U.S.Pharmacopeia. United States Pharmacopeial Convention, Rockville, MD.
U.S.Pharmacopeia, Tablet friability, 2019. In: Brown, W.E. (Ed.), U.S.Pharmacopeia. United States Pharmacopeial Convention, Rockville, MD.
Chadwick, K., Chen, J., Myerson, A.S., Trout, B.L., 2012. Toward the rational design of crystalline surfaces for heteroepitaxy: role of molecular functionality. Cryst Growth Des 12, 1159–1166.
Chauhan, S.L., Nathwani, S.V., Soniwala, M.M., Chavda, J.R., 2017. Development and characterization of multifunctional directly compressible co-processed excipient by spray drying method. AAPS PharmSciTech 18, 1293–1301.
U.S.Pharmacopeia, Acetaminophen Tablets, 2019. In: Clydewyn, A.M. (Ed.), U.S.Pharmacopeia. United States Pharmacopeial Convention, Rockville, MD.
Di Martino, P., Guyot-Hermann, A.M., Conflant, P., Drache, M., Guyot, J.C., 1996. A new pure paracetamol for direct compression: the orthorhombic form. Int J Pharm 128, 1–8.
Fell, J., Newton, J., 1970a. Determination of tablet strength by the diametral-compression test. J Pharm Sci 59, 688–691.
Fell, J., Newton, J., 1970b. Determination of tablet strength by the diametral-compression test. J Pharm Sci 59, 688–691.
Gad, S.C., 2008. Preclinical Development handbook: ADME and Biopharmaceutical Properties. John Wiley & Sons.
Garr, J.S.M., Rubinstein, M.H., 1991. An investigation into the capping of paracetamol at increasing speeds of compression. Int J Pharm 72, 117–122.
Gohel, M.C., Jogani, P.D., 2005. A review of co-processed directly compressible excipients. J Pharm Sci 8, 76–93.
Gonnissen, Y., Goncalves, S.I.V., De Geest, B.G., Remon, J.P., Vervaet, C., 2008. Process design applied to optimise a directly compressible powder produced via a continuous manufacturing process. Eur. J Pharm. and Biopharm 68, 760–770.
Gonnissen, Y., Remon, J.P., Vervaet, C., 2007. Development of directly compressible powders via co-spray drying. Eur J Pharm and Biopharm. 67, 220–226.
Govedarica, B., Injac, R., Srcic, S., 2009. Formulation and evaluation of immediate release tablets with different types of paracetamol powders prepared by direct compression. African J Pharm. and Pharma. 5, 31–41.
Gunsel, W.C., Lachman, L., 1963. Comparative evaluation of tablet formulations prepared from conventionally-processed and spray-dried lactose. J Pharm Sci 52, 178–182.
Heckel, R., 1961. Density-pressure relationships in powder compaction. Transactions of the Metallurgical Soc AIME 221, 671–675.
Hiestand, E.N., 1997. Mechanical properties of compacts and particles that control tableting success. J Pharm Sci 86, 985–990.
Hoag, S.W., Dave, V.S., Moolchandani, V., 2008. Compression and compaction. Pharmaceutical Dosage Forms-Tablets. CRC Press, pp. 571–646.
Hooper, D., Clarke, F., Mitchell, J., Snowden, M., 2016. A modern approach to the Heckel Equation: the effect of compaction pressure on the yield pressure of ibuprofen and its sodium salt. J Nanomedicine and Nanotechnol 7, 2.
Huang, Z., Scicolone, J.V., Han, X., Davé, R.N., 2015. Improved blend and tablet properties of fine pharmaceutical powders via dry particle coating. Int J Pharm 478, 447–455.
Iyer, R.M., Hegde, S., Dinunzio, J., Singhal, D., Malick, W., 2014. The impact of roller compaction and tablet compression on physicomechanical properties of pharmaceutical excipients. Pharm Dev Technol 19, 583–592.
Kaerger, J.S., Edge, S., Price, R., 2004. Influence of particle size and shape on flowability and compactibility of binary mixtures of paracetamol and microcrystalline cellulose. Eur. J Pharm Sce. 22, 173–179.
Khan, K.A., Rhodes, C.T., 1973. Production of tablets by direct compression. Canadian J. Pharm Sci. 8, 1–5.
Leuenberger, H., 2001a. New trends in the production of pharmaceutical granules: the classical batch concept and the problem of scale-up. Eur. J Pharm. and Biopharm. 52, 279–288.
Leuenberger, H., 2001b. New trends in the production of pharmaceutical granules: batch versus continuous processing. Eur. J Pharm and Biopharm. 52, 289–296.
Lindberg, N.-.O., 1988. Some experience of continuous granulation. Acta Pharm. Suec. 25, 239–246.
Maghsoodi, M., Taghizadeh, O., Martin, G.P., Nokhodchi, A., 2008. Particle design of naproxen-disintegrant agglomerates for direct compression by a crystallo-co-agglomeration technique. Int J Pharm 351, 45–54.
Mangal, S., Meiser, F., Morton, D., Larson, I., 2015. Particle engineering of excipients for direct compression: understanding the role of material properties. Current Pharmaceutical Design 21, 5877–5889.
McDonagh, A.F., Tajber, L., 2019. The control of paracetamol particle size and surface morphology through crystallisation in a spray dryer. Advanced Powder Technol. 31, 287–299.
McDonagh, A.F., Tajber, L., 2020. Crystallo-co-spray drying as a new approach to manufacturing of drug/excipient agglomerates: impact of processing on the properties of paracetamol and lactose mixtures. Int J Pharm 577, 119051.
McKenna, A., McCafferty, D.F., 1982. Effect of particle size on the compaction mechanism and tensile strength of tablets. J. Pharm and Pharmacology 34, 347–351.
G.W.B.E.T. Meggle, Technical brochure StarLac, in, 2014.
Moore, J., Flanner, H., 1996. Mathematical comparison of dissolution profiles. Pharmaceutical Technology 20, 64–74.
Newton, J.M., Haririan, I., Podczeck, F., 2000. The influence of punch curvature on the mechanical properties of compacted powders. Powder Technol 107, 79–83.
British-Pharmacopoeia, Disintigration testing, 2019. In: Office, T.S. (Ed.), British-Pharmacopoeia. Stationery Office.
Paczkowska, M., McDonagh, A.F., Bialek, K., Tajber, L., Cielecka-Piontek, J., 2020. Mechanochemical activation with cyclodextrins followed by compaction as an effective approach to improving dissolution of rutin. Int J Pharm 581, 119294.
Paradkar, A.R., Pawar, A.P., 2014. Crystallo-co-agglomeration: a novel particle engineering technique. Asian J Pharm. 4, 4–10.
Pawar, A.P., Paradkar, A.R., Kadam, S.S., Mahadik, K.R., 2004. Crystallo-co-agglomeration: a novel technique to obtain ibuprofen-paracetamol agglomerates. AAPS PharmSciTech 5, 57–64.
Pingali, K., Mendez, R., Lewis, D., Michniak-Kohn, B., Cuitino, A., Muzzio, F., 2011.

Mixing order of glidant and lubricant–influence on powder and tablet properties. Int J Pharm 409, 269–277.
Roberts, R.J., Rowe, R.C., 1985. The effect of punch velocity on the compaction of a variety of materials. J Pharm and Pharmacology 37, 377–384.
Rojas, J., Buckner, I., Kumar, V., 2012. Co-proccessed excipients with enhanced direct compression functionality for improved tableting performance. Drug Dev Ind Pharm 38, 1159–1170.
Shangraw, R.F., 1989. Compressed tablets by direct compression. Pharmaceutical dosage forms: Tablets 1, 195–246.
Shangraw, R.F., 1993. A survey of current industrial practices in the formulation and manufacture of tablets and capsules. Pharm. Technol 32, 32–44.
Sun, C.C., Grant, D.J.W., 2001. Influence of crystal structure on the tableting properties of sulfamerazine polymorphs. Pharm. Res. 18, 274–280.
Telford, R., Seaton, C.C., Clout, A., Buanz, A., Gaisford, S., Williams, G.R., Prior, T.J., Okoye, C.H., Munshi, T., Scowen, I.J., 2016. Stabilisation of metastable polymorphs: the case of paracetamol form III. Chemical Communications 52, 12028–12031.
Tye, C.K., Sun, C.C., Amidon, G.E., 2005. Evaluation of the effects of tableting speed on the relationships between compaction pressure, tablet tensile strength, and tablet solid fraction. J Pharm Sci 94, 465–472.
Vervaet, C., Remon, J.P., 2005. Continuous granulation in the pharmaceutical industry. Chem Eng Sci 60, 3949–3957.
Vromans, H., De Boer, A.H., Bolhuis, G.K., Lerk, C.F., Kussendrager, K.D., Bosch, H., 1985. Studies on tableting properties of lactose. Int J Clin Pharm 7, 186–193.
Yang, J.-J., Liu, C.-Y., Quan, L.-H., Liao, Y.-H., 2012. Preparation and in vitro aerosol performance of spray-dried Shuang-Huang-Lian corrugated particles in carrier-based dry powder inhalers. AAPS PharmSciTech 13, 816–825.
Zhang, Y., Huo, M., Zhou, J., Zou, A., Li, W., Yao, C., Xie, S., 2010. DDSolver: an add-in program for modeling and comparison of drug dissolution profiles. AAPS J 12, 263–271.